World Journal of Experimental Medicine

Submit a Manuscript: http://www.wjgnet.com/esps/
Help Desk: http://www.wjgnet.com/esps/helpdesk.aspx
DOI: 10.5493/wjem.v5.i2.140

World J Exp Med 2015 May 20; 5(2): 140-153
ISSN 2220-315X (online)

ORIGINAL ARTICLE

Clinical Trials Study

Barriers in contribution of human mesenchymal stem cells to murine muscle regeneration

Anabel S de la Garza-Rodea, Hester Boersma, Cheryl Dambrot, Antoine AF de Vries, Dirk W van Bekkum, Shoshan Knaän-Shanzer

Anabel S de la Garza-Rodea, Children's Hospital Oakland Research Institute, Oakland, CA 94609, United States
Hester Boersma, Dirk W van Bekkum, Shoshan Knaän-Shanzer, Virus and Stem Cell Biology Laboratory, Department of Molecular Cell Biology, Leiden University Medical Center, Leiden 2333 ZC, the Netherlands
Cheryl Dambrot, Yale School of Medicine, New Haven, CT 06510, United States
Antoine AF de Vries, Department of Cardiology, Leiden University Medical Center, Leiden 2333 ZC, the Netherlands
Author contributions: de la Garza-Rodea AS, Boersma H and Dambrot C performed experiments; de la Garza-Rodea AS, Boersma H, de Vries AAF and Knaän-Shanzer S analyzed the data; de la Garza-Rodea AS, van Bekkum DW and Knaän-Shanzer S designed the study and wrote the manuscript.
Supported by A scholarship to AS de la Garza-Rodea from the Universidad Autonoma de Nuevo Leon, Monterrey, Mexico.
Ethics approval: Approval from ethical committee obtained.

Correspondence to: Dr. Shoshan Knaän-Shanzer, Virus and Stem Cell Biology Laboratory, Department of Molecular Cell Biology, Leiden University Medical Center, Einthovenweg 20, Leiden 2333 ZC, the Netherlands. shoshanknaan@gmail.com
Telephone: +31-71-5269246
Fax: +31-62-4486785
Received: August 25, 2014
Peer-review started: August 26, 2014
First decision: October 14, 2014
Revised: December 27, 2014
Accepted: February 4, 2015
Article in press: February 9, 2015
Published online: May 20, 2015

Abstract

AIM: To study regeneration of damaged human and murine muscle implants and the contribution of added xenogeneic mesenchymal stem cells (MSCs).

METHODS: Minced human or mouse skeletal muscle tissues were implanted together with human or mouse MSCs subcutaneously on the back of non-obese diabetic/severe combined immunodeficient mice. The muscle tissues (both human and murine) were minced with scalpels into small pieces (< 1 mm^3) and aliquoted in portions of 200 mm^3. These portions were either cryopreserved in 10% dimethylsulfoxide or freshly implanted. Syngeneic or xenogeneic MSCs were added to the minced muscles directly before implantation. Implants were collected at 7, 14, 30 or 45 d after transplantation and processed for (immuno)histological analysis. The progression of muscle regeneration was assessed using a standard histological staining (hematoxylin-phloxin-saffron). Antibodies recognizing Pax7 and von Willebrand factor were used to detect the presence of satellite cells and blood vessels, respectively. To enable detection of the bone marrow-derived MSCs or their derivatives we used MSCs previously transduced with lentiviral vectors expressing a cytoplasmic *LacZ* gene. X-gal staining of the fixed tissues was used to detect β-galactosidase-positive cells and myofibers.

RESULTS: Myoregeneration in implants of fresh murine muscle was evident as early as day 7, and progressed with time to occupy 50% to 70% of the implants. Regeneration of fresh human muscle was slower. These observations of fresh muscle implants were in contrast to the regeneration of cryopreserved murine muscle that proceeded similarly to that of fresh tissue except for day 45 (P < 0.05). Cryopreserved human muscle showed minimal regeneration, suggesting that the freezing

procedure was detrimental to human satellite cells. In fresh and cryopreserved mouse muscle supplemented with LacZ-tagged mouse MSCs, β-galactosidase-positive myofibers were identified early after grafting at the well-vascularized periphery of the implants. The contribution of human MSCs to murine myofiber formation was, however, restricted to the cryopreserved mouse muscle implants. This suggests that fresh murine muscle tissue provides a suboptimal environment for maintenance of human MSCs. A detailed analysis of the histological sections of the various muscle implants revealed the presence of cellular structures with a deviating morphology. Additional stainings with alizarin red and alcian blue showed myofiber calcification in 50 of 66 human muscle implants, and encapsulated cartilage in 10 of 81 of murine muscle implants, respectively.

CONCLUSION: In mouse models the engagement of human MSCs in myoregeneration might be underestimated. Furthermore, our model permits the dissection of species-specific factors in the microenvironment.

Key words: Skeletal muscle; Muscle regeneration; Muscle implants; Mesenchymal stem cells; Satellite cells

Core tip: The translational relevance of animal models for tissue repair is often ambiguous. We describe here a murine model for the comparison of the regeneration of damaged human and murine skeletal muscle implants and the contribution of human and mouse mesenchymal stem cells (MSCs) to this process. Our findings suggest that murine muscle tissue provides a suboptimal environment for maintenance of human MSC, and that in mouse models their capacity to engage in myoregeneration is underestimated. The added value of the present model is that it permits the dissection of species-specific factors in the microenvironment.

de la Garza-Rodea AS, Boersma H, Dambrot C, de Vries AAF, van Bekkum DW, Knaän-Shanzer S. Barriers in contribution of human mesenchymal stem cells to murine muscle regeneration. *World J Exp Med* 2015; 5(2): 140-153 Available from: URL: http://www.wjgnet.com/2220-315X/full/v5/i2/140.htm DOI: http://dx.doi.org/10.5493/wjem.v5.i2.140

INTRODUCTION

The recent advances in (1) the derivation of human pluripotent stem cells; (2) the characterization and *ex vivo* amplification of human somatic stem cells; and (3) the genetic modification of these cells have created new prospects for cell-based therapies. The therapeutic potential of (engineered) human stem cells should ideally be validated in humans. Due to practical and ethical restrictions this type of study is, however, largely restricted to animals.

After transplantation of different human stem cell types including pericytes[1], satellite cells[1], mesenchymal stem cells (MSCs)[2] and muscle precursor cells[3] into damaged murine skeletal muscle, typically 1%-7% of the myofibers in the regenerated tissue contained human nuclei. Similar experiments performed with allogeneic satellite cells injected into muscles of mdx mice[4] (a mouse model for Duchenne muscular dystrophy) showed more than 10% chimeric myofibers after the administration of a significantly smaller cell dose than was used for the xenotransplantation studies. The reconstitution frequency by syngeneic donor cells was even more profound in mdx mice transplanted with a subpopulation of satellite cells with 94% of all myofibers becoming chimeric[5]. Although these findings require confirmation by direct comparative studies, they suggest a higher propensity of murine than of human (stem) cells to participate in the regeneration of mouse skeletal muscle tissue. Consequently, the results of preclinical studies with human stem cells in mice may lead to an underestimation of their therapeutic potential in humans.

The present study is an attempt to develop a method for investigating this assumption. This method is based on the free grafting together with human MSCs (hMSCs) or mouse MSCs (mMSCs) of minced human or mouse skeletal muscle implanted under the subcutis of mice. The reason to work with minced tissue was that it permits an even distribution of added MSCs throughout the implant. Successful free grafting of mammalian muscles was first accomplished in the 1960s[6]. As implants, either intact or minced skeletal muscle pieces have been used. Transplantation of these materials occurred into an emptied skeletal muscle bed or at a heterotopic anatomical site[7-10]. Under all conditions, myoregeneration was preceded by host-mediated vascularization and innervation[6,11] of the grafted tissue. We selected the subcutis as the site of implantation to preclude participation of host skeletal muscle cells in the regeneration of the graft[7,8,10]. The study includes both human and murine muscle grafts, both fresh and cryopreseved, supplemented with either mouse- or human bone marrow (BM)-derived MSCs. Non-obese diabetic/severe combined immunodeficient non-obese diabetic (NOD)/LtSz-scid/scid/J [in brief NOD/severe combined immunodeficient (SCID)] mice served as hosts.

MATERIALS AND METHODS

Skeletal muscle tissues

Human skeletal muscle specimens were collected from anonymous surgical "waste" material in orthopedic surgery. In agreement with the pertinent Leiden University Medical Center (LUMC; Leiden, the Netherlands) guidelines, and in accordance with the Best Practices code of Dutch Federation of Biomedical Scientific Societies, and the

based on article 467 of the "Wet op de Geneeskundige Behandelingsovereenkomst (WGBO)" no informed consent is required for the use of anonymous and non-traceable body materials and the institutional ethics committee of the LUMC waived the need for patient consent. The samples (from 53 patients, 26 females and 27 males, in an age-range of 26 to 82 years) were washed once with phosphate-buffered saline (PBS; Sigma-Aldrich, St. Louis, MO), freed of tendons and clumps of non-muscle tissue and chopped with scalpels into fragments < 1 mm^3.

Mouse skeletal muscle tissue was collected from all legs, dorsum and abdomen of 2 male- and 8 female-BALB/c (2 to 21 mo old) mice or 1 male-C57BL/6 (8 mo old) mouse (Harlan, Venray, the Netherlands), pooled and chopped with scalpels into fragments measuring < 1 mm^3.

Both human and mouse muscle mince were aliquoted in portions of 200 mm^3. These were either cryopreserved or freshly implanted within 3 h after collection.

The minced tissue aliquots used for preservation were suspended in ice-cold culture medium (see next section) supplemented with 10% dimethylsulfoxide (DMSO; Sigma-Aldrich), kept at -80 ℃ overnight and subsequently stored in liquid nitrogen vapor until use. Prior to implantation, the tissues were thawed and DMSO was removed by washing 3 times with PBS.

Isolation and culture of MSCs

hMSCs were isolated from BM of "waste" material collected according to the guidelines of the LUMC (mentioned above) during orthopedic surgery performed on a 38-year-old-female. Cells were isolated and cultured as previously described[12]. Cell expansion was performed in culture medium consisting of Dulbecco's modified Eagle's medium (DMEM) containing 4.5 g/L glucose, L-glutamine, sodium pyruvate, 100 U/mL penicillin, 100 μg/mL streptomycin, and 10% fetal bovine serum (FBS; all from Invitrogen, Breda, the Netherlands) and 0.5 ng/mL basic fibroblast growth factor (FGF2; Sigma-Aldrich) in CELLSTAR cell culture flasks (Greiner Bio-One, Frickenhausen, Germany) at 37 ℃ in humidified air containing 10% CO_2.

mMSCs were isolated from BM of 16-wk-old female-BALB/c mice and cultured under the same conditions as the hMSCs.

hMSCs at passage number 4 and mMSCs at passage number 6 were transduced with LV.EF1a.CMV.LacZ as previously described[2].

The tumorigenic potential of mMSCs of passage 14 was tested through subcutaneous injection of 10^6 cells in 2 male NOD/SCID of 8-wk-old. Animals sacrificed at 15 and 36 d after transplantation did not show any macroscopic alterations in primary organs and did not display abnormally growing cell masses at the site of injection (data not shown).

Animals and subcutaneous implants

Recipient mice for the human and BALB/c mouse muscle mince were NOD/SCID mice from a breeding colony established with animals from Jackson Laboratory (Bar Harbor, ME). In total 70 mice were used (43 females and 27 males) with an age range of 2 to 13 mo. C57BL/6-Tg (CAG + EGFP) C14-Y01-FM131Osb[13] recipient mice (4 females of 4 to 5 mo) of which almost all tissues including skeletal muscle expressed a recombinant enhanced green fluorescent protein (*eGFP*) gene were used to detect contribution of host cells to the regeneration of the muscle implants. These mice were obtained from Dr. Masaru Okabe, Osaka University, Japan and received donor skeletal muscle tissue from C57BL/6 mice (described above). All mice were kept in the Animal Facility of the LUMC following the internal guidelines. Experimentation with animals was performed in compliance with a protocol approved by the animal ethics committee of the LUMC.

Minced muscles of either human or mouse origin were implanted subcutaneously on the back of the mouse. Routinely, each NOD/SCID mouse received two implants, one of human and one of murine origin, to minimize variability caused by recipient-associated conditions. Grafting was performed under aseptic conditions and general anesthesia with isoflurane. The back of the mouse was shaved and rinsed with ethanol. Next, two longitudinal 1-cm incisions to the left and right of the spine were made with a scalpel. The incisions were enlarged using scissors (Fine Science Tools, CA, United States) dissecting the skin from dorsal fascia thus forming a dermal pocket in which a standard volume of 200 mm^3 minced muscle tissue alone or thoroughly mixed with 5×10^5 MSCs was deposited. The MSCs were always freshly harvested from cultures in logarithmic growth phase. The wound was closed with two or three ETHICON PROLENE polypropylene size 5-0 sutures (Johnson and Johnson Medical, Amersfoort, the Netherlands). After 7, 14, 30 or 45 d mice were sacrificed by cervical dislocation, the implants were removed and processed for (immuno)histological analyses.

Tissue processing and (immuno)histochemistry

The excised implants were cut in two halves and fixed either overnight at 4 ℃ or for 1 h at room temperature in 4% buffered formaldehyde (Mallinckrodt Baker, Phillipsburg, NJ). Tissues fixed at room temperature were stained with X-gal (Sigma-Aldrich) as previously described[2].

All samples were embedded in paraffin, cut into 6-μm-thick sections and consecutive sections were placed on SuperFrost Plus slides (Menzel-Gläser, Braunschweig, Germany) for histochemical and immunohistological staining.

Tissue sections of each sample were deparaffinized, rehydrated with graded ethanol-water mixtures and stained with hematoxylin (Klinipath BV, Duiven, Netherlands), phloxin (Sigma-Aldrich) and saffron (Ghohestan, Iran) (HPS) following standard procedures.

After dehydration, the sections were mounted with Pertex mounting medium (Histolab Products, Gothenburg, Sweden).

Direct microscopical screening of HPS-stained sections revealed in some implants areas reminiscent of bone and cartilage. Consecutive sections of those implants were stained with Alizarin Red S or Alcian Blue (both from Sigma-Aldrich) to visualize calcium deposits and sulfated glycosaminoglycans, respectively. Staining was performed on deparaffinized tissue sections, which were incubated for 2 min with Alizarin Red S or for 30 min with Alcian Blue. The Alcian Blue-stained sections were rinsed with water and counterstained for 5 min with Nuclear Fast Red (Sigma-Aldrich). Sections treated with either protocol were twice rinsed with water prior to dehydration and mounting on slides with Pertex mounting medium.

Immunohistology was used to assess myoregeneration as based on the presence of myoblast and/or multi-nucleated myofibers that stain positive for desmin; satellite cells that stain positive for Pax7; blood vessels detected by von Willebrand Factor (vWF) and LacZ labelled cells and their derivatives (beta Gal).

Tissue sections were deparaffinized, rehydrated and boiled for 10 min in 10 mmol/L citrate buffer (Sigma-Aldrich, pH = 6.0) for antigen retrieval. After rinsing the slides with water, endogenous peroxidase was inactivated by a 10-min incubation at room temperature with 0.3% (w/w) hydrogen peroxide (Sigma-Aldrich) in water. Following two additional washes with PBS a 1 h blocking step was performed using 10% normal goat serum (Dako Netherlands, Heverlee, Belgium) in PBS. Next, mouse monoclonal antibodies specific for desmin (clone D33; IgG1, κ; Dako Netherlands, dilution 1:100) or directed against chicken Pax7 (IgG1, κ; Developmental Studies Hybridoma Bank, University of Iowa, Iowa City, IA; dilution 1:20) or the rabbit polyclonal anti-human vWF antiserum (that interacts with murine cells; Dako Netherlands; dilution 1:3000; also binds murine vWF) were added to sections for an overnight incubation at 4 ℃. The following day, the sections were washed in PBS and the secondary antibodies, either horseradish peroxidase-linked goat anti-mouse IgG (Dako Netherlands; dilution 1:100) or horseradish peroxidase-conjugated goat anti-rabbit IgG (Dako Netherlands; dilution 1:100) were applied for 30 min. The binding of the antibodies was visualized with 3,3'-diaminobenzidine (DAB; Sigma-Aldrich). The sections were counterstained with hematoxylin, dehydrated and mounted with Pertex mounting medium. Images were captured with a Color View IIIu camera mounted on an Olympus BH-2 microscope and processed using CELL^F imaging software (all from Olympus Nederland, Zoeterwoude, Netherlands).

For the detection of eGFP-positive satellite cells an eGFP-specific rabbit polyclonal antiserum was used together with the aforementioned murine anti-Pax7 monoclonal antibody. Deparaffinized and rehydrated tissue sections were immersed twice in 10 mmol/L citric acid solution (pH = 6.0) for 5 min at 90 ℃. Following cooling and washing steps the sections were blocked for 2 to 3 h with 4% IgG- and protease-free bovine serum albumin (Jackson ImmunoResearch Europe, Newmarket, United Kingdom) in PBS. Next, the sections were sequentially incubated with goat anti-mouse IgG (H + L) AffiniPure Fab fragment (MouseFab, Jackson ImmunoResearch; dilution 0.05 mg/mL) for 30 min, with the anti-Pax7 antibody overnight, with biotin-SP-conjugated AffiniPure goat anti-mouse IgG (H + L) (Jackson ImmunoResearch; dilution 1:20) for 45 min and with Cy3-conjugated streptavidin (Jackson ImmunoResearch, dilution 1:1250) for 30 min. Each incubation step was followed by three rinses with PBS. The sections were re-blocked with MouseFab for 30 min and labeled overnight with eGFP-specific rabbit polyclonal antiserum (IgG fraction; Invitrogen; dilution 1:200) followed by Alexa 488-linked donkey anti-rabbit IgG (H + L) antibodies (Invitrogen; dilution 1:200) for 1 h. Next, the sections were stained for 10 min at room temperature with 1 μg/mL of Hoechst 33342 (Invitrogen) in PBS, washed thrice with PBS to remove excess dye and mounted in Vectashield mounting medium (Vector Laboratories, Burlingame, CA). Light microscopic analysis was performed with a Leica DM5500 B fluorescence microscope (Leica Microsystems, Rijswijk, the Netherlands). Images were captured with a CoolSNAP K4 CCD camera (Photometrics, Tuscon, AZ) and archived using home-made software.

Statistical analysis

Results are expressed as mean ± SD. The level of statistical significance was determined by one- or two-way analysis of variance (ANOVA) followed by Bonferroni's *t* test for multiple comparisons, using Prism software (GraphPad Software Inc., San Diego, CA). A P value < 0.05 was considered significant.

RESULTS

Regeneration of ectopically implanted fresh human and mouse skeletal muscle tissue

In an initial experiment designed to set up the model, the regeneration kinetics of fresh human and BALB/c mouse muscle mince implanted under the skin of NOD/SCID mice were compared starting at day 7 after grafting when the implant is well-vascularized[14,15].

The histological images of multiple tissue sections of the excised implants stained with HPS were used to visualize the morphology and composition of the implants.

In all cases the implants were encapsulated by dense connective tissue as identified by the light orange saffron stain (Figure 1A and 1B1). The central part of the implants consisted generally of anuclear myofibers (Figure 1C11 and 15) a characteristic of myofiber degeneration. In sections labeled with the desmin-specific antibody, areas of skeletal muscle regeneration[16] could be distinguished from non-

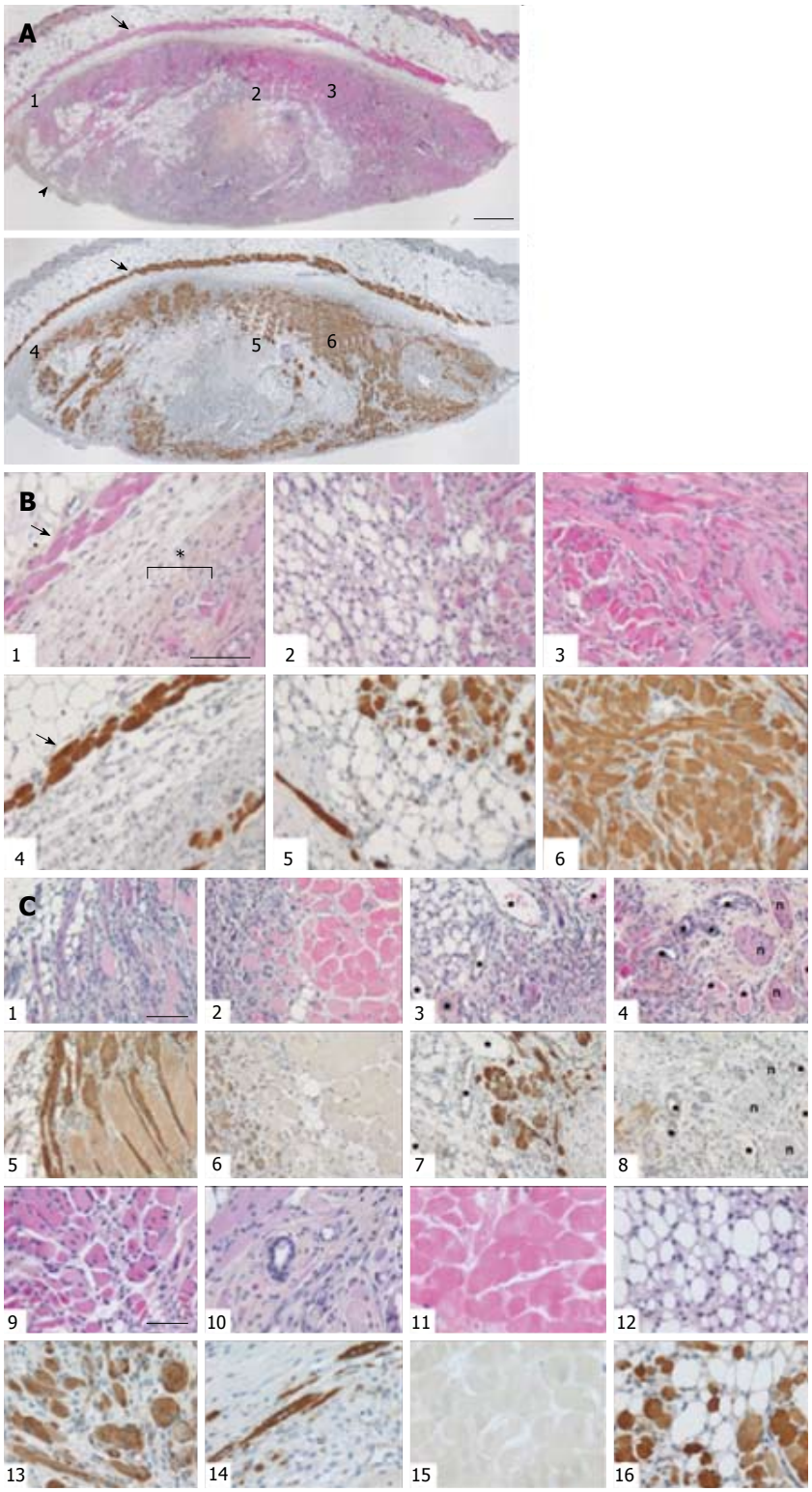

Figure 1 Histological analysis of subcutaneous murine muscle implants. A: Representative images of HPS-stained (upper panel) and desmin-stained (lower panel) sections of a cryopreserved mouse mince muscle implant at 30 d after implantation. From top to bottom are visible the skin layers (epidermis, dermis and hypodermis), the panniculus carnosus muscle (PC, arrow), a thin layer of connective tissue surrounding the implant (light yellow, arrowhead) and tissues composing the implant (*e.g.*, adipose, skeletal muscle, nerves and other tissues). The intense brown desmin stain (lower panel) identifies myofibers of the PC (host) and myoblasts as well as regenerating myofibers of the implant. Scale bar is 500 μm; B: Higher magnifications of the marked areas in A. (1 and 4), connective tissue encapsulating the implant (asterisk). Arrows indicate PC. (2 and 5), adipose tissue and myoblast/myofibers in the central part of the implant. (3 and 6), areas of regeneration with myofibers positioned at different angles. Scale bar is 100 μm; C: Exemplary areas showing specific cells and structures as observed both in fresh and cryopreserved implants. For each pair of images the upper panels correspond to HPS- and desmin-stained tissue sections, respectively. (1, 5, 2 and 6), myoblasts and newly formed myofibers of different sizes and positioned at different angles. (3, 7, 4 and 8), blood vessels (asterisks) and nerves (n) usually located at the edges of the implants. (9, 13, 10 and 14), areas of active regeneration with centronucleated myofibers of different sizes. (11 and 15), degenerated myofibers devoid of nuclei and desmin. (12 and 16), myoregeneration within an adipogenic area. Scale bar is 100 μm for 1-8 and 50 μm for 9-16 is 50 μm. Note the images of HPS- and desmin-stained tissue sections do not always show overlapping areas.

regenerating areas in the implants by the intense brown staining of myoblasts and myofibers (Figure 1B4, 5 and 6). Myoregeneration typically started at the periphery of the implants within the well vascularized connective tissue (see below) and extended with time towards the center (Figure 1B3 and 6). In the areas of myoregeneration satellite cells (Figure 2A), myoblasts and multinucleated myofibers of different sizes and irregularly distributed were observed (Figure 1B3 and 6, 1C1 and 4).

To investigate the vascularization of the implants, sections were immunostained for the endothelial cell marker vWF. Small blood vessels and capillaries staining positive for the endothelial cell marker vWF (Figure 3) were identified as early as at day 7 only in the periphery of the implants but later also in the inner parts. All implants also contained adipose and fibrotic tissues albeit in different amounts and at a different

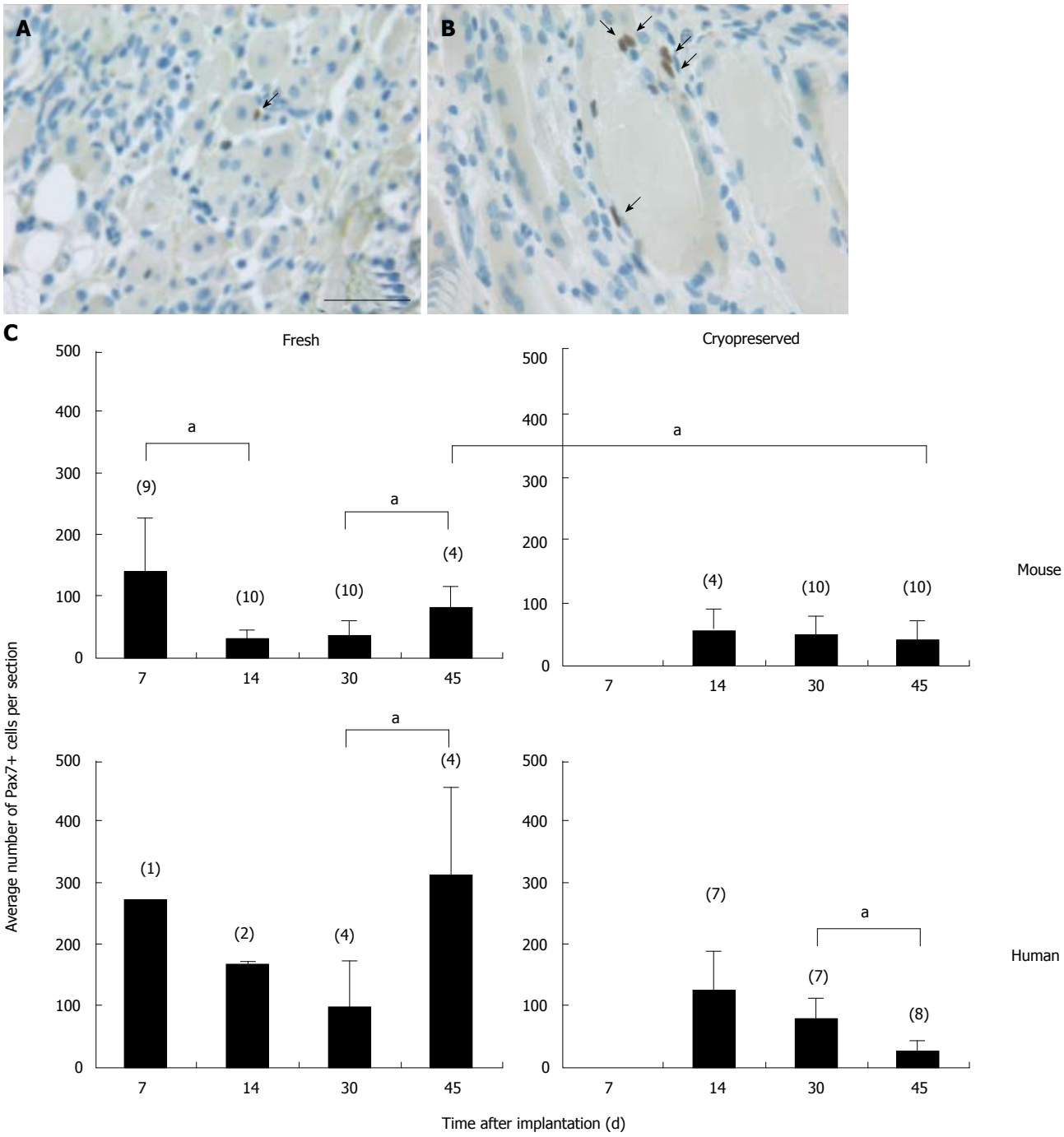

Figure 2 Pax7$^+$ cells in regenerating skeletal muscle implants. A, B: Examples of single (A and B) and pairs of (B) Pax7$^+$ cells (arrows) attached or positioned in close proximity to myofibers in a fresh mouse implant at 14 d after implantation. Scale bar is 50 μm; C: Pax7$^+$ cell counts in cross sections of fresh and cryopreserved mouse and human implants. From the center of each implant two or three consecutive sections were stained for Pax7. The average number of Pax7$^+$ cells per section and SD are plotted. Data from implants with or without MSCs were pooled as they contained very similar numbers of Pax7$^+$ cells. Numbers in parentheses indicate numbers of implants analyzed. [a]$P < 0.05$.

distribution (Figures 1 and 4). In general, large differences in the quantities of adipose tissue, fibrotic tissue and skeletal muscle tissue (degenerating and regenerating) were observed even between implants derived from the same donor.

A chronological study of myoregeneration revealed differences in the progression of this process between human and murine implants (Figure 5).

In the fresh mouse muscle implants, shortly after transplantation (day 7), the thin peripheral rim of regenerated tissue consisted predominantly of mononucleated myoblasts. Progression of the regenerative process was evident by the occurrence of elongated multinucleated myofibers at days 14 and 30 post transplantation (Figure 4). The regenerating area gradually extended to occupy 50% to 70% of the implants (Figure 5) Pax7$^+$ cells were detected in all implants, mostly in the periphery. Their number

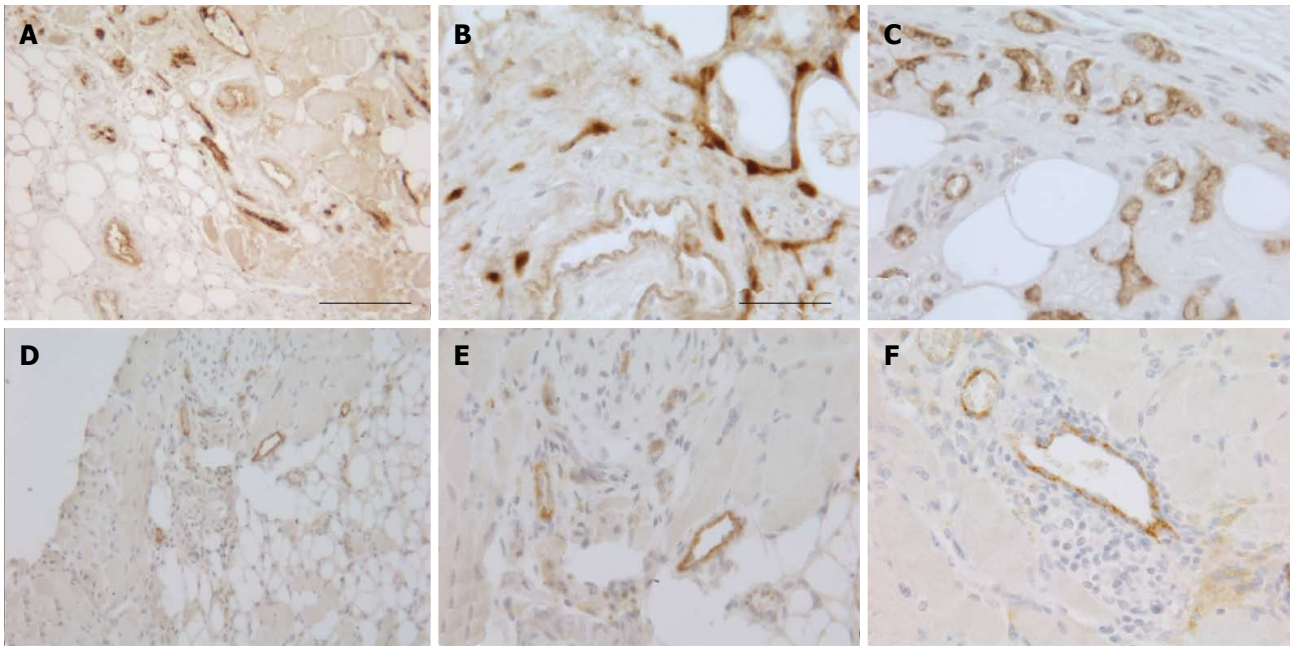

Figure 3 Vascularization of subcutaneous skeletal muscle implants. Photomicrographs of sections of fresh human (A-C) and mouse (D-F) minced implants at 30 d after transplantation stained for vWF (brown). Scale bar is 100 μm for (A, D) and 50 μm for (B, C, E, F).

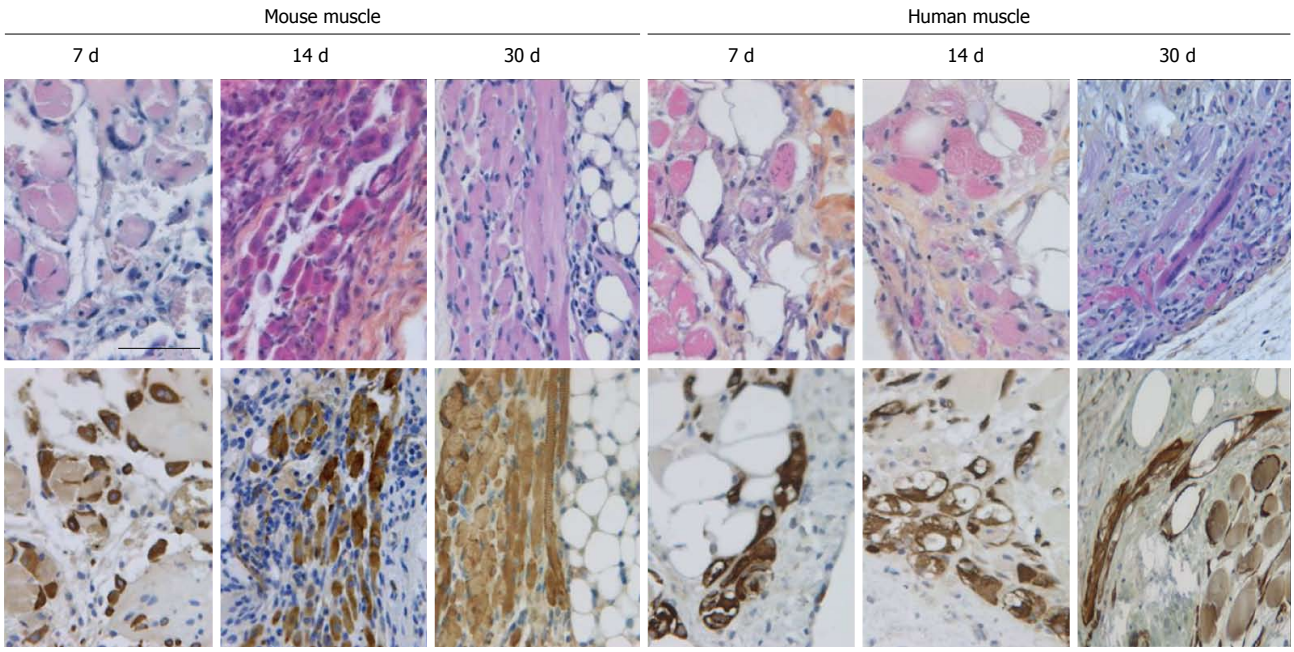

Figure 4 Myoregeneration of mouse and human minced cryopreserved muscle implants. Mouse and human fresh muscle implants were excised at different time points and stained with HPS (upper panels) or for desmin (lower panels). In the mouse implants progression of myoregeneration over time from myoblasts to small and large myofibers was evident. In the human implants, fewer myoblast/myofibers were identified at all time points. Scale bar is 50 μm.

in murine donor tissue was highest at day 7 after implantation (Figure 2C). The observed decrease in the number of $Pax7^+$ cells at later time points (day 30) coincided with an increase in myoregeneration in the fresh murine muscle implants (compare Figure 2C with Figure 5).

The regeneration process in the fresh human muscle implants resembled that in the murine implants, albeit at a slower rate (Figures 4 and 5). The extent of regeneration as deduced from the number of myoblasts and regenerated myofibers in the human tissue at day 30 and 45 after implantation was lower than in the murine muscle at day 14 post transplantation. Notably, the number of satellite (*i.e.*, $Pax7^+$) cells in the human muscle implants was twice to four times as high as that observed in the murine muscle tissue (Figure 2C).

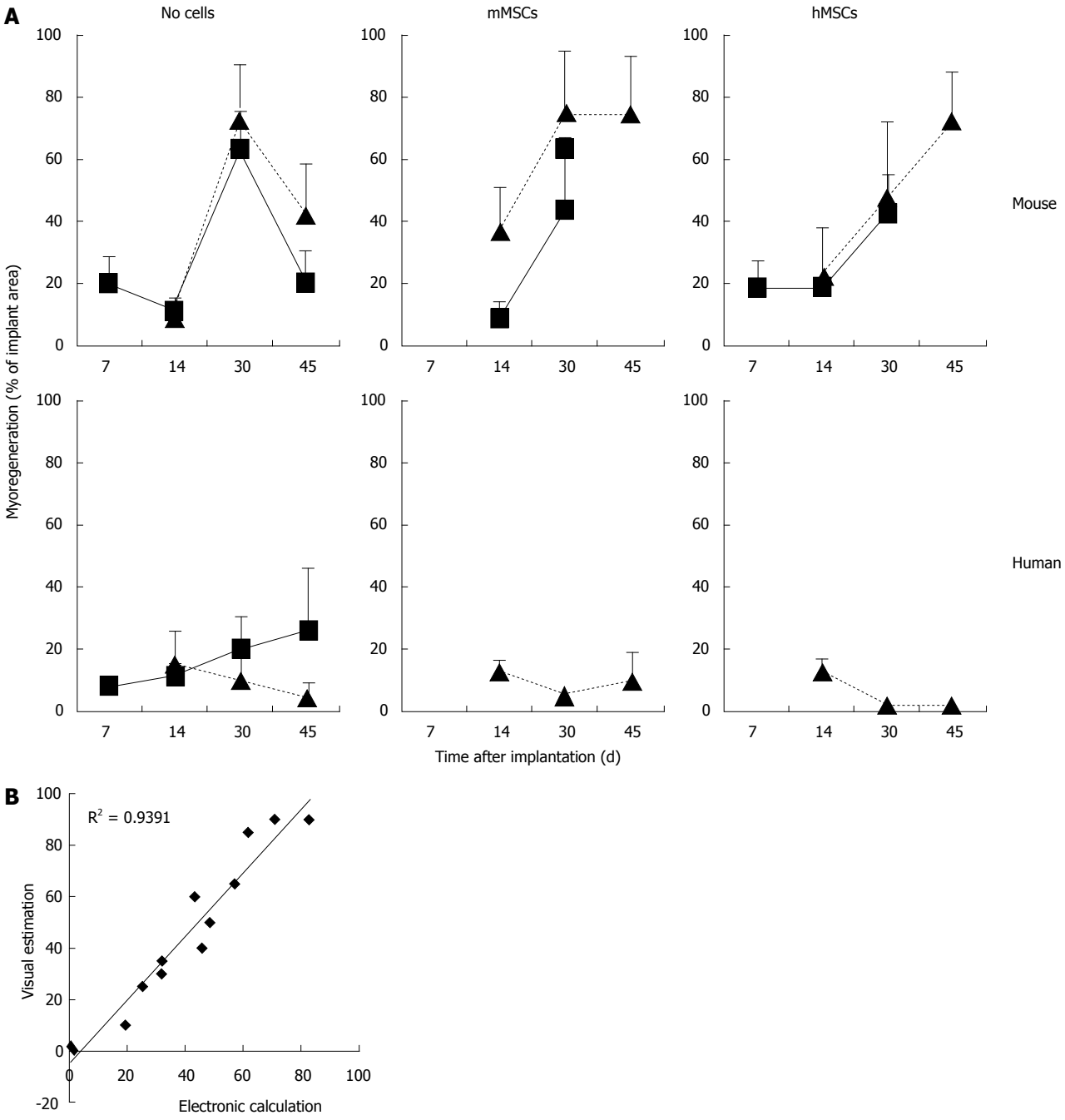

Figure 5 Myoregeneration kinetics of minced muscle implants without and with mesenchymal stem cells. A: The data represent visual estimates derived from microscopic examination of 2 or 3 desmin-stained sections through the center of fresh (square frame and solid line) and cryopreserved (triangle and broken line) implants. Each point represents the mean with SD of between 2 and 10 (average 4) implants; B: Comparison between visual estimation and electronic calculation of areas of myoregeneration. Thirteen desmin-stained cross sections were analyzed by both visual estimation (plotted on the Y-axis) and with the Interactive Image Measurement program of CELL^F imaging software (plotted on the X-axis). The excellent correlation between the two methods of analysis justifies the choice of the less laborious visual estimation procedure.

Regeneration of cryopreserved muscle tissue

Because of the logistic problems caused by the irregular supply of human muscle samples and their limited size, we explored the option of using cryopreserved tissue. This approach allows also pooling of samples collected at different dates and from different donors, a strategy that might improve reproducibility.

The regeneration of cryopreserved mouse muscle closely resembled that of the fresh implants as judged by HPS and desmin stainings (Figure 4). The frequency of $Pax7^+$ cells (Figure 2C) was not much affected by the freezing procedure, except for day 45 ($P < 0.05$). Human muscle cryopreserved in an identical manner behaved differently. At 14 d after transplantation, the ingrowth of capillaries into the implant and signs of myoregeneration were observed at the edges of the donor tissue like in implants of fresh tissue. At later time points (days 30 and 45),

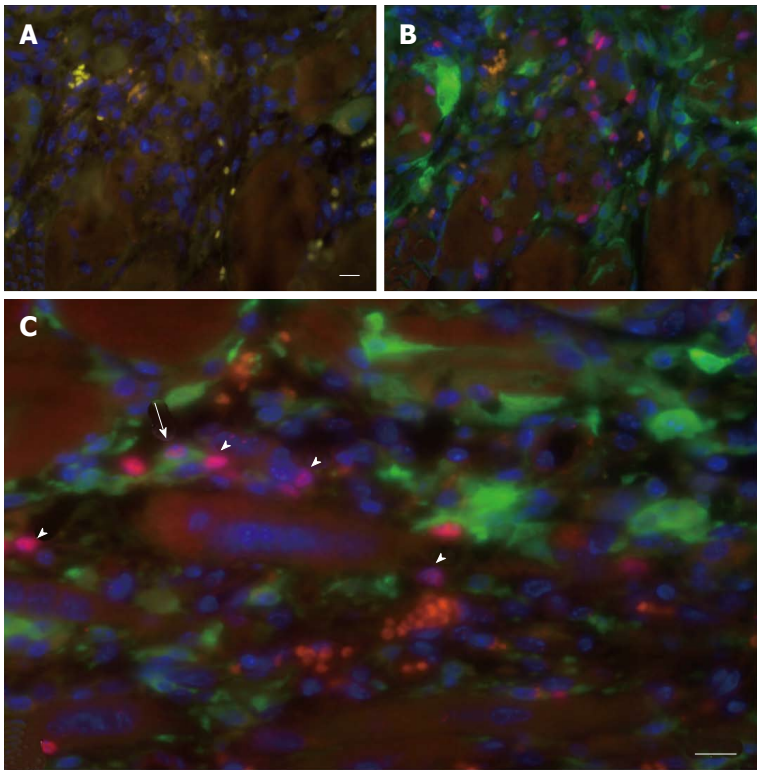

Figure 6 Contribution of host cells to myoregeneration in the muscle implant. Immunofluorescence analysis of a fresh mouse implant excised 7 d after implantation in eGFP transgenic recipients. Host cell contribution was evaluated in tissue sections stained with the karyophilic fluorochrome Hoechst 33342 and antibodies specific for eGFP and Pax7. A: Negative control section incubated with Hoechst 33342 (blue), the secondary antibodies and Cy3-conjugated streptavidin; B: Section stained for Pax7 (red), eGFP (green) and Hoechst 33342 (blue); C: Example of a cell positive for both Pax7 and eGFP (arrow) situated at the periphery of the implant. Also present are cells only positive for Pax7 (arrowheads) or for GFP, blood vessels with erythrocytes (orange) and multinucleated myofibers (center of image). Scale bar for a and b is 50 μm. Panel (C) shows an electronic enlargement of an image recorded at the same magnification as (A) and (B).

however, the implants from frozen tissue consisted mostly of fibrotic and/or adipose tissue. Degenerating muscle tissue gradually disappeared while the level of newly formed myoblasts/myofibers remained low (Figure 4). In contrast to the fresh muscle implants, the number of satellite cells decreased with time (Figure 2B), suggesting damage to the satellite cell population by the preservation procedure.

Contribution of host cells to myoregeneration in subcutaneous muscle implants

The skin of a mouse, like that of most rodents, contains a thin skeletal muscle layer named the panniculus carnosus. As some damage of the panniculus carnosus during the implantation procedure is unavoidable, a possible contamination of the graft with recipient satellite cells had to be taken into consideration. This was investigated using eGFP-expressing transgenic hosts that were implanted with skeletal muscle tissue of syngeneic C57BL/6 mice. The minced muscle implants were analyzed 7 d later for the presence of eGFP+ cells expressing Pax7, indicative for contamination of the implant with host-derived satellite cell. A large number of eGFP+ mononucleated cells was present in the implants but only a few isolated cells co-expressed Pax7 (Figure 6). These findings demonstrate a negligible contribution of recipient cells to the myoregenerative process in the implants and are in agreement with previous reports[7,17].

The evident profusion of erythrocytes and host-derived mononuclear cells in the implants underlines the functional vascularization of the graft already early after transplantation.

Effect of syngeneic or xenogeneic MSCs on myoregeneration in muscle implants

Addition of BM-derived LacZ-tagged MSCs of either species to minced muscle tissue (fresh or cryopreserved) prior to implantation did not consistently affect the degree or the kinetics of myoregeneration to any significant extent (Figure 5A).

The presence of MSCs in the implants and their contribution to the myofiber formation was evaluated using sections stained with 5-bromo-4-chloro-3-indolyl-D-galactopyranoside (X-gal). β-galactosidase-positive (b-gal+, blue color) cells were present generally in all sections. Their frequency, distribution, and incorporation into multinucleated myofibers were different in the various implants. To enable comparison between the different treated groups we used an arbitrary score ranging from 0 to 4, where (0) no blue cells; (1) single blue cells only; (2) in addition clusters of blue cells; (3) in addition clusters of blue cells and some blue myofibers; and (4) in addition clusters of blue myofibers. The persistence of MSCs and their participation in myofiber formation were similar for the mMSC and the hMSC in cryopreserved murine muscle implants as well as for mMSC in fresh mouse muscle implants. In contrast, hMSCs were strikingly less abundant in implants of fresh mouse muscle and did not contribute to myofiber formation at any time points (Figure 7A). While numerous blue myofibers were recorded in implants supplemented with syngeneic MSCs, only isolated blue cells were detected in the implants supplemented with the xenogeneic cells (Figure 7B). The higher contribution of the mMSCs as compared to the hMSCs is in line with findings in the

cardiotoxin (CTX)-damage *in vivo* mouse model of the tibialis anterior muscle[2] where hMSCs were half as effective in producing β-gal+ myofibers as mMSCs (Figure 7C).

The contribution of MSCs to human skeletal muscle regeneration could only be investigated in cryopreserved muscle. Supplementation of the implants with mMSCs or hMSCs did not lead to the formation of β-gal+ myofibers at any of the time points (Figure 7A). Under all conditions, MSCs persisted in the implants as isolated or clustered mononuclear cells (score 2 or lower).

Myofiber calcification and cartilage formation in subcutaneous muscle implants

A thorough analysis of the histological sections of the various muscle implants revealed the presence of cellular structures with a deviating morphology. Additional specific staining with Alizarin Red S confirmed calcification of myofibers in 50 of 66 analyzed human muscle implants (Figure 8A1, 2 and B). This calcification, which occurred predominantly in degenerated myofibers, was seen in implants of both fresh and cryopreserved human muscle tissue either supplemented or not with MSCs.

In 10 of 81 of the murine muscle implants we identified isolated islands of encapsulated cartilage (Figure 8A3, 4 and B) by staining with Alcian Blue. This occurred in implants with as well as without MSCs. Calcification has not been recorded in any of the murine implants. Similarly, we have not found chondrogenesis in the human muscle implants at any time point.

DISCUSSION

A major impediment to the development of stem cell therapy for myogenic disorders is the paucity of models for studying regeneration of human skeletal muscle. The minced muscle implants described here have provided information of translational significance: firstly, by confirming *in vivo* observations[18] that regeneration perse is slower for human muscle than for murine muscle, and secondly, by demonstrating that MSCs have little or no effect on the rate of myoregeneration. This observation corroborates previous findings from our research group with human BM-derived MSCs and CTX-injured murine tibialis anterior muscles[2]. Thirdly, by revealing that the contribution of hMSCs to the regeneration of fresh mouse muscle implants is far below that of implants of cryopreserved murine muscle, suggesting that the results obtained with the current *in vivo* models, which are based on the direct injection of hMSCs into damaged mouse muscle, their myoregenerative capacity in humans may be underestimated. Based on this finding it is tempting to speculate that species-specific inhibitors in the mouse tissue that become deactivated by the cryopreservation may be present. This model, may, then, offer excellent opportunities for identifying such inhibitors and evaluating their significance for tissue regeneration.

Furthermore, the contribution of MSCs to myofiber formation seems to occur only in tissues undergoing massive myoregeneration, like the murine implants at 30 and 45 d post transplantation. In tissues showing no or little evidence of regeneration, like the cryopreserved human muscle implants at day 30 after transplantation, β-gal+ myofibers were not detected. The observation that MSCs are maintained in the damaged muscle environment as mononucleated cells without contributing to the active satellite cell pool or forming homotypic myofibers may argue against MSCs having autonomous myogenic differentiation capacity. The β-gal+ myofibers observed in the murine implants result solely from fusion of MSCs with nascent or regenerating implant-derived myofibers.

This conclusion is in line with the notion that the intrinsic differentiation potential of MSCs is limited to certain connective cell types including osteoblasts, chondrocytes, adipocytes, fibroblasts and adventitial reticular cells[19,20]. Evidence provided so far for the ability of MSCs to differentiate along the myogenic lineage is conflicting. Although some previous studies assigned myogenic properties to MSCs by demonstrating their *in vitro* and *in vivo* differentiation into satellite cells and myoblasts and their ability to form myotube-like structures through homotypic fusion[19,21], others regard the myogenic reprogramming of the MSCs to be the consequence of their fusion with inherently myogenic cells[2,22,23]. Whether this contradiction can be attributed to the differences in MSC origin, the model used or the read-out methods applied, remains to be investigated.

Implantation experiments revealed that cryopreservation was detrimental to the recovery of human satellite cells but not to that of the murine cells. Regeneration of cryopreserved murine muscle was the same as that of fresh tissue. These results were rather unexpected. Such difference was not recorded between human and murine cells of other tissues (*e.g.*, hematopoietic stem cells and MSCs). To take this study forward, efforts will have to be made to improve human satellite cell viability and proliferation potential. In the development of the cryopreservation protocols reduction of the concentration of DMSO or even its omission from the preservation mixtures should be considered, according to a recent report[24].

The finding of hyaline cartilage in the murine implants and calcified myofibers in the human muscle implants, was both intriguing and has so far not been described. The myofiber calcification without evident bone-like trabeculae formation, that was observed in 75% of the human muscle implants, may represent dystrophic calcification that often occurs in necrotic soft tissues[25,26]. The rapid onset of myoregeneration in the murine muscle implants and its progression through the entire implant, leaving only few degenerating myofibers, might explain the absence of calcification in the murine implants.

The origin of the cartilage, however, is more difficult

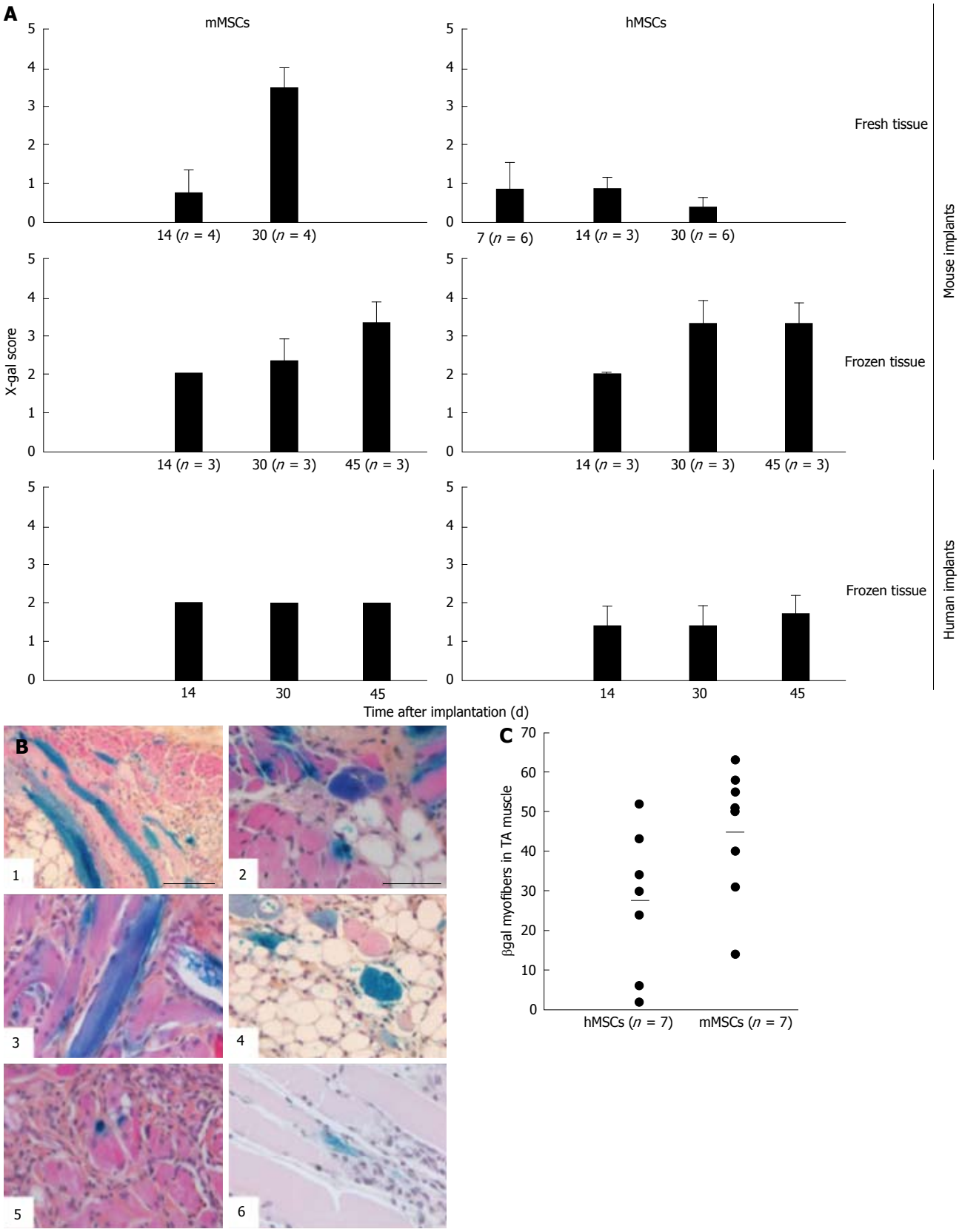

Figure 7 Contribution of mouse mesenchymal stem cells and human mesenchymal stem cells to myoregeneration in implants of fresh and cryopreserved mouse and human muscle minced. MSCs and their derivatives were identified by X-gal staining. A: For comparing implants we used an arbitrary score described in Results. Plotted in A is the average X-gal score and SD. Numbers in parentheses indicate number of implants analyzed; B: Representative images of X-gal-stained sections of fresh mouse muscle implants at 30 d after grafting. Note the higher frequency of blue myofibers (longitudinal and transversal cuts) and β-gal$^+$ mononuclear cells in the implants containing mMSCs (B1-4) as compared to those with hMSCs (B5 and 6). Scale bar is 100 μm for B1 and 50 μm for B2 through B6; C: Quantification of β-gal$^+$ myofibers in CTX-damaged tibialis anterior (TA) muscles of NOD/SCID mice following injection of LacZ-tagged MSCs. Each mouse received 5 × 10^5 cells. Muscles were collected 30 d after stem cell injection and processed as described in[2]. Data points represent numbers of hybrid myofibers per TA. The average number of hybrid myofibers for hMSCs and mMSCs was 27 ± 18.3 and 45 ± 16.2, respectively. MSCs: Mesenchymal stem cells; hMSCs: Human mesenchymal stem cells; mMSCs: Mouse mesenchymal stem cells.

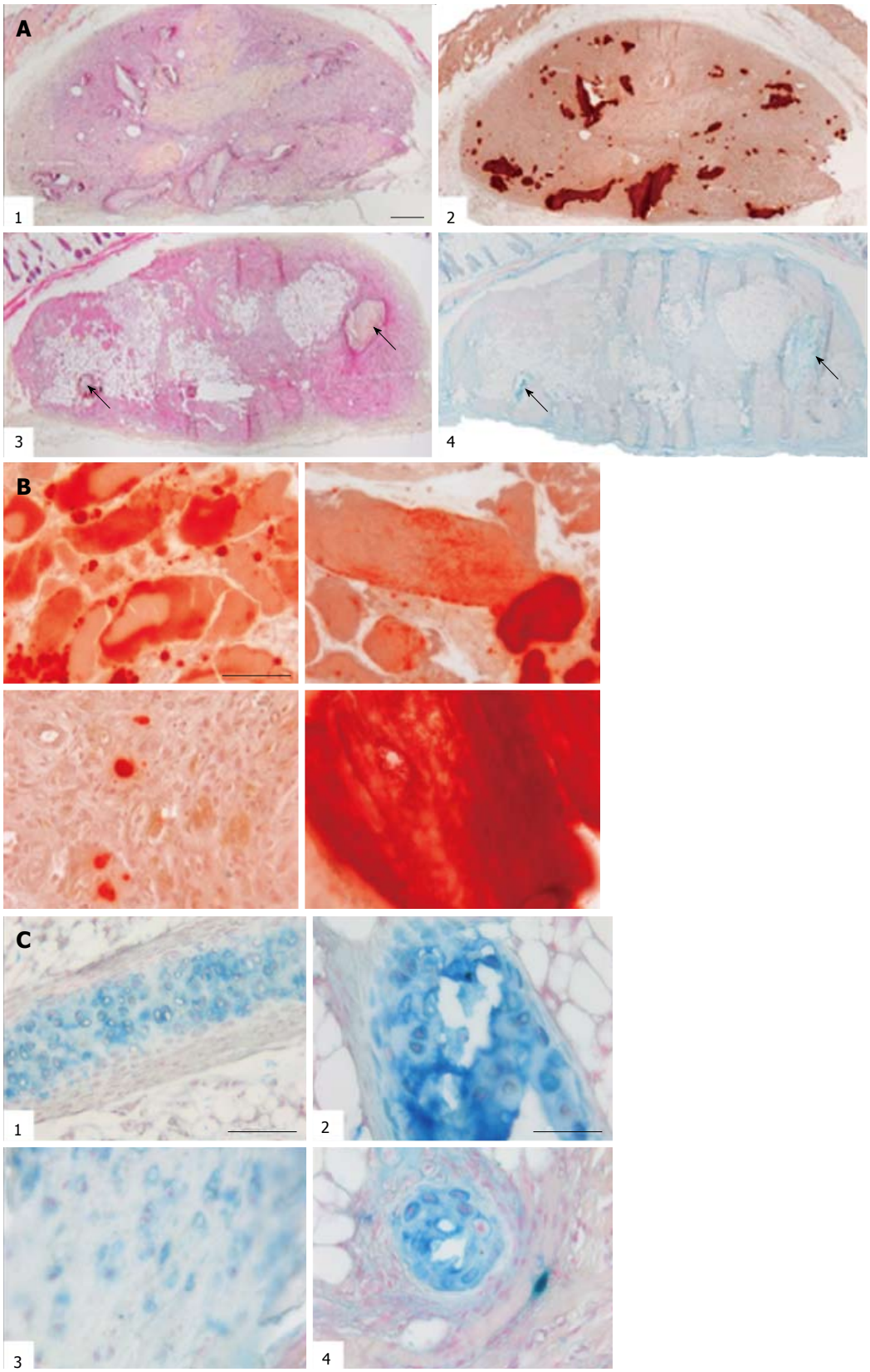

Figure 8 Myofiber calcification and cartilage formation in skeletal muscle implants. A: Human (1, 2) and murine (3, 4) muscle implants at 30 d after grafting stained with HPS (1, 3), Alizarin Red S for bone (2) or Alcian Blue for cartilage (4). Arrows indicate cartilage. Scale bar is 500 μm; B: Larger magnifications of Alizarin Red S-stained myofibers in human muscle implants. Scale bar is 50 μm; C: Larger magnifications of Alcian Blue-stained murine implants. (1), mouse sternum (positive control for the staining procedure), (2-4), examples of chondrogenic tissue in murine muscle grafts. Scale bar is 100 μm for (1) and 50 μm for (2-4).

to explain. It was often seen within the adipose tissue of the implants an environment that, to our knowledge, has not been reported for aberrant cartilage formation before.

In summary, our primary question of whether the contribution of MSCs to myoregeneration is subject to species barriers could be partly answered through the use of ectopically implanted minced muscle. While hMSCs failed to participate in the regeneration of fresh mouse muscle implants, they did contribute to the regeneration of murine skeletal muscle tissue that had been cryopreserved prior to implantation. Collectively, our data indicate that the *in vivo* model described herein is valuable for studying some aspects of human skeletal muscle degeneration and regeneration. A major practical issue to be tackled is the cryopreservation of human skeletal muscle for which the current standard technique was found to fail.

COMMENTS

Background

The translational relevance of animal models for tissue repair is often ambiguous. The authors describe here a murine model for the comparison of the regeneration of damaged human and murine skeletal muscle implants and the contribution of human and mouse mesenchymal stem cells (MSCs) to this process. These cells were mixed with minced muscle prior to subcutaneous implantation in mice, this allows for an equal distribution of the MSCs in the muscle mass. The added value of the present model is that it permits the dissection of species-specific factors in the microenvironment.

Research frontiers

The recent advances in (1) the derivation of human pluripotent stem cells; (2) the characterization and *ex vivo* amplification of human somatic stem cells; and (3) the genetic modification of these cells have created new prospects for cell-based therapies. A major impediment to the development of stem cell therapy for myogenic disorders is the paucity of animal models for studying regeneration of human skeletal muscle.

Innovations and breakthroughs

After transplantation of different human stem cell types including pericytes, satellite cells, MSCs and muscle precursor cells into damaged murine skeletal muscle, typically 1%-7% of the myofibers in the regenerated tissue contained human nuclei. Similar experiments performed with allogeneic satellite cells injected into muscles of mdx mice (a mouse model for Duchenne muscular dystrophy) showed more than 10% chimeric myofibers after the administration of a significantly smaller cell dose than was used for the xenotransplantation studies. The reconstitution frequency by syngeneic donor cells was even more profound in mdx mice transplanted with a subpopulation of satellite cells with 94% of all myofibers becoming chimeric. Although these findings require confirmation by direct comparative studies, they suggest a higher propensity of murine than of human (stem) cells to participate in the regeneration of mouse skeletal muscle tissue. Consequently, the results of preclinical studies with human stem cells in mice may lead to an underestimation of their therapeutic potential in humans. The present study is an attempt to develop a method for investigating this hypothesis.

Applications

These findings suggest that fresh murine muscle tissue provides a suboptimal environment for maintenance of human MSC, and that in *in vivo* mouse models their capacity to engage in myoregeneration is underestimated. The added value of the present model is that it permits the dissection of species-specific factors in the microenvironment. The broader application of this model requires the development of improved methods to cryopreserve satellite cells in human skeletal muscle.

Terminology

The study includes both human and murine muscle grafts, both fresh and cryopreseved, supplemented with either mouse- or human bone marrow-derived MSCs. Non-obese diabetic/severe combined immunodeficient mice served as hosts. Implantation of minced muscle was subcutaneous (under the skin) that facilitates tracking of implant and its removal.

Peer-review

The study conducted by de la Garza-Rodea *et al* described a murine model using subcutaneous implants of minced muscle for examining the regeneration of damaged human and murine skeletal muscle implants and the contribution of added corresponding human and mouse mesenchymal stem cells. The authors concluded that (1) the contribution of human mesenchymal stem cells to murine myofiber formation was restricted to the cryopreserved mouse muscle implants suggesting that fresh murine muscle tissue provided a suboptimal environment for the maintenance of human mesenchymal stem cells; and (2) their described model allowed the dissection of species-specific factors in the microenvironment. The authors commented that the application of their described model requires the development of improved methods to cryopreserve satellite cells in human skeletal muscle.

REFERENCES

1 **Dellavalle A**, Sampaolesi M, Tonlorenzi R, Tagliafico E, Sacchetti B, Perani L, Innocenzi A, Galvez BG, Messina G, Morosetti R, Li S, Belicchi M, Peretti G, Chamberlain JS, Wright WE, Torrente Y, Ferrari S, Bianco P, Cossu G. Pericytes of human skeletal muscle are myogenic precursors distinct from satellite cells. *Nat Cell Biol* 2007; **9**: 255-267 [PMID: 17293855 DOI: 10.1038/ncb1542]

2 **de la Garza-Rodea AS**, van der Velde I, Boersma H, Gonçalves MA, van Bekkum DW, de Vries AA, Knaän-Shanzer S. Long-term contribution of human bone marrow mesenchymal stromal cells to skeletal muscle regeneration in mice. *Cell Transplant* 2011; **20**: 217-231 [PMID: 20719081 DOI: 10.3727/096368910X522117]

3 **Bouchentouf M**, Benabdallah BF, Mills P, Tremblay JP. Exercise improves the success of myoblast transplantation in mdx mice. *Neuromuscul Disord* 2006; **16**: 518-529 [PMID: 16919954 DOI: 10.1016/j.nmd.2006.06.003]

4 **Ikemoto M**, Fukada S, Uezumi A, Masuda S, Miyoshi H, Yamamoto H, Wada MR, Masubuchi N, Miyagoe-Suzuki Y, Takeda S. Autologous transplantation of SM/C-2.6(+) satellite cells transduced with micro-dystrophin CS1 cDNA by lentiviral vector into mdx mice. *Mol Ther* 2007; **15**: 2178-2185 [PMID: 17726457 DOI: 10.1038/sj.mt.6300295]

5 **Cerletti M**, Jurga S, Witczak CA, Hirshman MF, Shadrach JL, Goodyear LJ, Wagers AJ. Highly efficient, functional engraftment of skeletal muscle stem cells in dystrophic muscles. *Cell* 2008; **134**: 37-47 [PMID: 18614009 DOI: 10.1016/j.cell.2008.05.049]

6 **Studitsky AN.** Free auto- and homografts of muscle tissue in experiments on animals. *Ann N Y Acad Sci* 1964: 789-801

7 **Grounds MD**, Partridge TA. Isoenzyme studies of whole muscle grafts and movement of muscle precursor cells. *Cell Tissue Res* 1983; **230**: 677-688 [PMID: 6850788 DOI: 10.1007/BF00216211]

8 **Grounds M**, Partridge TA, Sloper JC. The contribution of exogenous cells to regenerating skeletal muscle: an isoenzyme study of muscle allografts in mice. *J Pathol* 1980; **132**: 325-341 [PMID: 7441406 DOI: 10.1002/path.1711320404]

9 **Gulati AK**, Rivner MH, Shamsnia M, Swift TR, Sohal GS. Growth of skeletal muscle from patients with amyotrophic lateral sclerosis transplanted into nude mice. *Muscle Nerve* 1988; **11**: 33-38 [PMID: 3340099 DOI: 10.1002/mus.880110107]

10 **Wakayama Y**, Schotland DL, Bonilla E. Transplantation of human skeletal muscle to nude mice: a sequential morphologic study. *Neurology* 1980; **30**: 740-748 [PMID: 7190240 DOI: 10.1212/WNL.30.7.740]

11 **Irintchev A**, Rosenblatt JD, Cullen MJ, Zweyer M, Wernig A. Ectopic skeletal muscles derived from myoblasts implanted under the skin. *J Cell Sci* 1998; **111** (Pt 22): 3287-3297 [PMID: 9788871]

12 **Knaän-Shanzer S**, van de Watering MJ, van der Velde I, Gonçalves MA, Valerio D, de Vries AA. Endowing human adenovirus serotype 5 vectors with fiber domains of species B greatly enhances gene transfer into human mesenchymal stem cells. *Stem Cells* 2005; **23**: 1598-1607 [PMID: 16293583 DOI: 10.1634/stemcells.2005-0016]

13 **Okabe M**, Ikawa M, Kominami K, Nakanishi T, Nishimune Y. 'Green mice' as a source of ubiquitous green cells. *FEBS letters*

1997; **407**: 313-319 [DOI: 10.1016/S0014-5793(97)00313-X]
14 **Calcagni M**, Althaus MK, Knapik AD, Hegland N, Contaldo C, Giovanoli P, Lindenblatt N. In vivo visualization of the origination of skin graft vasculature in a wild-type/GFP crossover model. *Microvasc Res* 2011; **82**: 237-245 [PMID: 21784083 DOI: 10.1016/j.mvr.2011.07.003]
15 **Hathout E**, Chan NK, Tan A, Sakata N, Mace J, Pearce W, Peverini R, Chinnock R, Sowers L, Obenaus A. In vivo imaging demonstrates a time-line for new vessel formation in islet transplantation. *Pediatr Transplant* 2009; **13**: 892-897 [PMID: 19017287 DOI: 10.1111/j.1399-3046.2008.01088.x]
16 **Gallanti A**, Prelle A, Moggio M, Ciscato P, Checcarelli N, Sciacco M, Comini A, Scarlato G. Desmin and vimentin as markers of regeneration in muscle diseases. *Acta Neuropathol* 1992; **85**: 88-92 [PMID: 1285499 DOI: 10.1007/BF00304637]
17 **Washabaugh CH**, Ontell MP, Ontell M. Nonmuscle stem cells fail to significantly contribute to regeneration of normal muscle. *Gene Ther* 2004; **11**: 1724-1728 [PMID: 15385949 DOI: 10.1038/sj.gt.3302353]
18 **BM C.** In: Freilinger G HJ, Carlson BM Muscle transplantation. Wien: Springer-Vienna, 1981: 3-18
19 **Bianco P**, Robey PG, Saggio I, Riminucci M. "Mesenchymal" stem cells in human bone marrow (skeletal stem cells): a critical discussion of their nature, identity, and significance in incurable skeletal disease. *Hum Gene Ther* 2010; **21**: 1057-1066 [PMID: 20649485 DOI: 10.1089/hum.2010.136]
20 **Bianco P**, Robey PG, Simmons PJ. Mesenchymal stem cells: revisiting history, concepts, and assays. *Cell Stem Cell* 2008; **2**: 313-319 [PMID: 18397751 DOI: 10.1016/j.stem.2008.03.002]
21 **Liu Y**, Yan X, Sun Z, Chen B, Han Q, Li J, Zhao RC. Flk-1+ adipose-derived mesenchymal stem cells differentiate into skeletal muscle satellite cells and ameliorate muscular dystrophy in mdx mice. *Stem Cells Dev* 2007; **16**: 695-706 [PMID: 17999592 DOI: 10.1089/scd.2006.0118]
22 **Gonçalves MA**, Swildens J, Holkers M, Narain A, van Nierop GP, van de Watering MJ, Knaän-Shanzer S, de Vries AA. Genetic complementation of human muscle cells via directed stem cell fusion. *Mol Ther* 2008; **16**: 741-748 [PMID: 18334989 DOI: 10.1038/mt.2008.16]
23 **Shi D**, Reinecke H, Murry CE, Torok-Storb B. Myogenic fusion of human bone marrow stromal cells, but not hematopoietic cells. *Blood* 2004; **104**: 290-294 [PMID: 15010375 DOI: 10.1182/blood-2003-03-0688]
24 **Larsen S,** Wright-Paradis C, Gnaiger E, Helge JW, Boushel R. Cryopreservation of human skeletal muscle impairs mitochondrial function. *Cryo letters* 2012; **33**: 170-176
25 **Zhao P**, Caretti G, Mitchell S, McKeehan WL, Boskey AL, Pachman LM, Sartorelli V, Hoffman EP. Fgfr4 is required for effective muscle regeneration in vivo. Delineation of a MyoD-Tead2-Fgfr4 transcriptional pathway. *J Biol Chem* 2006; **281**: 429-438 [PMID: 16267055 DOI: 10.1074/jbc.M507440200]
26 **Zhao Y**, Urganus AL, Spevak L, Shrestha S, Doty SB, Boskey AL, Pachman LM. Characterization of dystrophic calcification induced in mice by cardiotoxin. *Calcif Tissue Int* 2009; **85**: 267-275 [PMID: 19690791 DOI: 10.1007/s00223-009-9271-5]

P- Reviewer: Puntel RL, Sugawara I, Siu PM **S- Editor**: Song XX
L- Editor: A **E- Editor**: Lu YJ

Published by **Baishideng Publishing Group Inc**
8226 Regency Drive, Pleasanton, CA 94588, USA
Telephone: +1-925-223-8242
Fax: +1-925-223-8243
E-mail: bpgoffice@wjgnet.com
Help Desk: http://www.wjgnet.com/esps/helpdesk.aspx
http://www.wjgnet.com